Acta Cryst. (1991). B47, 905–910

Electron-Density Distribution of 4-Hydroxy-1,2-benzisothiazol-3(2*H*)-one 1,1-Dioxide Sodium Salt (UH-AF 50 NA)

By R. Rudert, J. Buschmann, T. Richter and P. Luger

Institut für Kristallographie der Freien Universität Berlin, Takustraße 6, D-1000 Berlin 33, Germany

and G. Trummlitz

Dr K. Thomae GmbH, Birkendorfer Straße 65, D-7950 Biberach, Germany.

(*Received* 2 *April* 1990; *accepted* 11 *June* 1991)

Abstract

$Na^+.C_7H_4NO_4S^-.H_2O$, $M_r = 239{\cdot}2$, orthorhombic, *Pnam*, $a = 10{\cdot}844$ (4), $b = 12{\cdot}038$ (4), $c = 6{\cdot}903$ (3) Å, $V = 901{\cdot}1$ (9) Å^3, λ(Mo $K\alpha$) = 0·71069 Å, $Z = 4$, $D_x = 1{\cdot}762$ Mg m^{-3}, $\mu = 0{\cdot}389$ mm^{-1}, $F(000) = 488$, $T = 123$ K. Two data sets were used in refinements: one low-order data set ($\sin\theta/\lambda < 0{\cdot}8$ Å^{-1}): $R(F^2) = 0{\cdot}045$, $wR(F^2) = 0{\cdot}063$, and one high-order data set ($\sin\theta/\lambda > 0{\cdot}9$ Å^{-1}): $R(F^2) = 0{\cdot}058$, $wR(F^2) = 0{\cdot}064$. Experimental electron deformation density maps are calculated by difference Fourier synthesis. They are compared with theoretical 6-31G* deformation density maps of the isothiazolone ring fragment of the title compound. Theoretical and experimental deformation density maps show the influence of the Na^+ cation on the lone-pair density of the carbonyl oxygen atom.

Introduction

This work is part of a program to investigate the structure and electron-density distribution of saccharin derivatives with different taste properties. One aim of the program is to look for correlations between taste quality on the one hand and structure and/or electron deformation density, especially in the region of the assumed 'glucophore' of the isothiazolone ring, on the other. The 'glucophore' consists either of one of the SO_2 oxygen atoms and the nitrogen atom or of the nitrogen atom and the carbonyl oxygen atom. It is believed that the 'glucophore' forms a hydrogen-bonded complex with a receptor molecule, causing sweet or bitter taste. To estimate whether the experimental electron density is comparable to the electron density of the isolated molecule theoretical densities were calculated and compared with the experimental ones.

In two previous papers (Rudert, Buschmann, Luger, Gregson & Trummlitz, 1988, 1989) the neutron structures of the title compound and of 6-nitrosaccharin have been published. Now, the first electron-density study of a sweet-tasting saccharin derivative is presented and discussed.

Experimental

A crystal of approximate dimensions 0·7 × 0·28 × 0·24 mm was grown from an aqueous solution. The crystal was mounted in a glass capillary on an automatic Siemens four-circle diffractometer and cooled to 123 K by a cold nitrogen gas stream surrounded by a warm N_2 gas stream preventing the formation of ice near the crystal. The temperature at the crystal site was calibrated using a phase transition occurring in KH_2PO_4 at 123 K. It was reproducible within ± 1 K. The cell dimensions were calculated by least-squares refinement of 16 centered reflections with $36 < 2\theta < 54°$. X-ray reflection intensities were collected with Zr-filtered Mo $K\alpha$ radiation using an $\omega/2\theta$ step scan technique. The step size was 0·03° in ω, the scan width was $\Delta\omega(\theta) = (1{\cdot}41 + 0{\cdot}25\tan\theta)°$ for the first part of the measurement and $\Delta\omega(\theta) = (1{\cdot}29 + 0{\cdot}25\tan\theta)°$ for the second. The minimum and maximum counting times per step were 0·3 and 2·4 s, respectively.

A total of 6001 reflection intensities were collected, $0 \leq h \leq 17$, $-19 \leq k \leq 0$, $0 \leq l \leq 11$, of which 4931 were independent. 4110 unique reflections were considered observed [$F > 2\sigma(F)$]. Maximum $(\sin\theta)/\lambda$ was 1·053 Å^{-1}. Two standard reflections were remeasured every 30 min. Whenever the intensity of at least one of the standard reflections dropped by more than 2%, a new orientation matrix was calculated on the basis of 20 recentered reflections. Owing to difficulties with the attenuation filters, the measurement of the low-order data with $(\sin\theta)/\lambda < 0{\cdot}8$ Å^{-1} was repeated on the same crystal. The ω step size in this case was 0·02°, the scan width $\Delta\omega(\theta) = (1{\cdot}42 + 0{\cdot}25\tan\theta)°$. 2082 reflections were measured of which 1858 were considered observed. An absorption correction was carried out using the program *ABSORB* of the *XTAL* system (Stewart & Hall,

0108-7681/91/060905-06$03.00 © 1991 International Union of Crystallography

Table 1. *Refinements*

	(I) (Neutron)	(II) (X-ray)	(III) (X-ray)
$(\sin\theta)/\lambda$ range (Å^{-1})	0·0–0·651	0·0–0·803	0·90–1·053
N_{obs}	937	1858	1399
N_V	124	106	89
$R(F^2)$	0·079	0·045	0·058
$wR(F^2)$	0·110	0·063	0·064
S	4·8	3·36	1·11

1986). Correction factors were between 1·078 and 1·105, $0·0179 < \bar{t} < 0·0298$ cm.

Least-squares refinement

$wR(F^2) = [\sum w(F_o^2 - kF_c^2)^2/\sum wF_o^2]^{1/2}$ with $w = 1/\sigma^2(F^2)$ was minimized by full-matrix least-squares refinement using *SFLSX* in the *XTAL* system. Anomalous-dispersion corrections were applied for Na and S; the values were taken from *International Tables for X-ray Crystallography* (1974, Vol. IV). The form factors for the non-H atoms were taken from the same source, while for the H atoms those of Stewart, Davidson & Simpson (1965) were used.

Two refinements were carried out, designated as refinements (II) and (III) [refinement (I): neutron data]. In refinement (II) reflections with $\sin\theta/\lambda \leq 0·803$ Å^{-1} (second measurement) were used. Positional parameters of all atoms, anisotropic displacement parameters of the non-H atoms, isotropic values for the H atoms and an isotropic extinction parameter were refined (model by Zachariasen, 1967). In refinement (III) the high-order data with $\sin\theta/\lambda > 0·90$ Å^{-1} of the first measurement were used. The minimum F_c extinction correcting factor was 0·85. Starting values for the atomic parameters were taken from the neutron structure of UH-AF 50 NA (Rudert, Buschmann, Luger, Gregson & Trummlitz, 1988). Since the H atoms do not scatter sufficiently at high angles, their positional and displacement parameters were fixed during the high-order refinement to the values obtained from the neutron measurement. The extinction parameter of refinement (II) was used and kept fixed. Reliability factors of the two refinements are compared with those of the neutron data refinement in Table 1.*

Refinement of high-order data only [refinement (III)] gave a lower goodness of fit than the refinement of the low-order data set [refinement (II)]. The *R* values are larger due to the lower accuracy of the rather weak high-order reflections. Atomic positions of refinement (III) are shown in Table 2 along with the equivalent displacement parameters. Bond lengths and angles are shown in Table 3 and Fig. 1. Compared to the neutron structure all atoms are displaced with an average positional shift based on refinement (III) of 0·0064 Å which is of the order of magnitude of the standard deviations. The non-H atoms with the largest shifts are Na^+ [0·0224 Å away from O(3) and O(5)], C(3) [0·0113 Å away from O(3)], and C(8) (0·0083 Å towards the ring center).

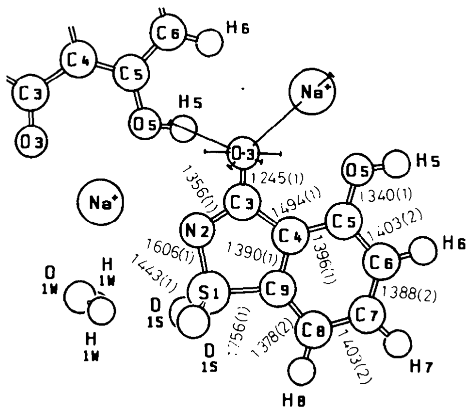

Fig. 1. *SCHAKAL*88 plot (Keller, 1988) of UH-AF 50 NA [refinement (III)]. Bond lengths in Å, e.s.d.'s in parentheses. For comparison with Fig. 2 part of another asymmetric unit is shown. The solid lines through O(3) mark the projections of the maps in Figs. 2, 3 and 4.

Table 2. *Atomic coordinates and equivalent isotropic displacement parameters* (Å^2 × 10^2), *refinement* (III)

	x	*y*	*z*	U_{eq}
Na	0·90459 (5)	−0·36582 (5)	¼	1·21 (1)
S(1)	0·66082 (2)	0·05649 (2)	¼	0·992 (9)
O(1S)	0·61451 (8)	0·10907 (7)	0·0768 (1)	1·82 (1)
N(2)	0·63329 (8)	−0·07465 (7)	¼	1·44 (2)
C(3)	0·73981 (8)	−0·13365 (7)	¼	1·15 (2)
O(3)	0·74197 (8)	−0·23708 (6)	¼	1·57 (2)
C(4)	0·85308 (7)	−0·06305 (7)	¼	1·08 (2)
C(5)	0·97753 (8)	−0·09274 (7)	¼	1·21 (2)
O(5)	1·00989 (7)	−0·20015 (7)	¼	1·63 (2)
C(6)	1·0655 (1)	−0·0072 (1)	¼	1·61 (2)
C(7)	1·0313 (1)	0·1039 (1)	¼	1·90 (3)
C(8)	0·9066 (1)	0·13495 (8)	¼	1·73 (2)
C(9)	0·82248 (8)	0·04914 (7)	¼	1·23 (2)
O(1*W*)	0·3565 (1)	0·06574 (9)	¼	2·00 (2)

Table 3. *Bond angles* (°), *with standard deviations in parentheses, for refinement* (III)

O(1S)—S(1)—O(1S)	112·05 (5)	O(1*S*)—S(1)—C(9)	111·67 (4)
C(9)—S(1)—N(2)	97·82 (4)	S(1)—N(2)—C(3)	110·87 (7)
N(2)—C(3)—C(4)	113·76 (8)	C(3)—C(4)—C(9)	110·84 (7)
C(4)—C(9)—S(1)	106·71 (6)	N(2)—C(3)—O(3)	122·76 (9)
O(3)—C(3)—C(4)	123·59 (8)	C(3)—C(4)—C(5)	130·51 (8)
C(5)—C(4)—C(9)	118·64 (8)	C(4)—C(5)—O(5)	120·02 (8)
C(4)—C(5)—C(6)	118·01 (8)	O(5)—C(5)—C(6)	121·97 (8)
C(5)—C(6)—C(7)	121·7 (1)	C(6)—C(7)—C(8)	120·9 (1)
C(7)—C(8)—C(9)	116·0 (1)	S(1)—C(9)—C(8)	128·57 (8)
C(4)—C(9)—C(8)	124·72 (9)		

---

* Lists of anisotropic displacement parameters and observed and calculated X-ray structure factors have been deposited with the British Library Document Supply Centre as Supplementary Publication No. SUP 54312 (58 pp.). Copies may be obtained through The Technical Editor, International Union of Crystallography, 5 Abbey Square, Chester CH1 2HU, England.

Table 4. *Overall rigid-body-motion parameters related to crystal axes*

Libration tensor in deg^2, vibration tensor in 100 Å^2.

L_{11}	L_{22}	L_{33}	L_{12}
1·6 (9)	0·2 (8)	2·7 (7)	− 1·4 (5)
T_{11}	T_{22}	T_{33}	T_{12}
0·9 (1)	0·7 (1)	2·1 (1)	−0·10 (9)

Table 5. *Hydrogen-bond distances* (Å) *and angles* (°) *for refinement* (III)

X—H···Y	X···Y	X—H	H···Y	X—H···Y	Symmetry operation for Y
O(1W)—H(1W)···O(1S)	3·087 (2)	0·947 (8)	2·374 (7)	131.9 (5)	$x, y, \frac{1}{2} - z$
O(5)—H(5)···O(3)	2·628 (2)	0·998 (7)	1·649 (7)	166·0 (5)	$\frac{1}{2} + x, \frac{1}{2} - y, z$

Table 6. Na$^+$ *coordination distances* (Å) *for refinement* (III) *with neutron data for comparison*

Na$^+$—Y			Symmetry operation for Y
Na$^+$—O(3)	2·348 (1)	2·332 (7)	x, y, z
Na$^+$—O(5)	2·298 (1)	2·274 (8)	x, y, z
Na$^+$—O(1W)	2·462 (2)	2·490 (8)	$\frac{1}{2} + x, -\frac{1}{2} + y, z$
Na$^+$—N(2)	2·582 (1)	2·586 (7)	$\frac{1}{2} + x, -\frac{1}{2} - y, z$
Na$^+$—O(1S)	2·285 (1)	2·291 (4)	$\frac{3}{2} - x, -\frac{1}{2} + y, \frac{1}{2} + z$
Na$^+$—O(1S′)	2·285 (1)	2·291 (4)	$\frac{3}{2} - x, -\frac{1}{2} + y, -\frac{1}{2} + z$

The equivalent displacement parameters of the non-H atoms from the X-ray measurement are larger than those of the neutron measurement by an average factor of 1·31. A rigid body has been fitted to the individual displacement parameters (Schomaker & Trueblood, 1968) (Table 4). A large thermal vibration was found in the direction of the c axis.

The OH···O hydrogen-bond distances are the same as in the neutron refinement (see Table 5). As a result of the above-mentioned shift of the sodium cation the Na$^+$ contact distances are different from those of the neutron measurement. The maximum difference is found for Na$^+$···O(1W) and is 0·0028 Å (Table 6).

Experimental and theoretical electron-density maps

A deformation density, $\Delta\rho = \rho_{\rm obs}/k - \sum\rho_{\rm spherical\ atom}$ was calculated. The positional and displacement parameters were taken from the high-order refinement. The observed deformation density was calculated using the low-order data set. As a compromise between reducing noise in the deformation density map and getting a maximum of information in the lone-pair regions, $\sin\theta/\lambda$ was limited to 0·70 Å^{-1}. The scale factor was obtained by refining k using the low-order data with all other parameters fixed.

Fig. 2 shows the deformation density in the plane of the UH-AF 50 NA molecule, which is also the crystallographic mirror plane, and in the plane defined by O(1S), S(1), and O(1S′). Peaks are found between all covalently bonded atoms in the planes, the peak heights ranging from 0·2 to 0·6 e Å^{-3}. Lone-pair peaks of N(2), O(3) and O(5) are also visible. Negative deformation density at the positions of Na$^+$, O(1W) and S(1) is most probably the result of partial positive charge at these atoms. Electron deficits at the center of S have also been observed in other sulfur-containing compounds (*e.g.*, Wang & Liao, 1988). The lone-pair peaks of O(1S) are shown in an extra section of Fig. 2.

We have calculated the theoretical electron deformation density of the UH-AF 50 anion and the 2,3-dihydroisothiazol-3-one 1,1-dioxide anion (the fragment of UH-AF 50 with the phenyl ring omitted). In a third calculation we evaluated the electron deformation density of this fragment plus one sodium atom and one water molecule near the isothiazolone oxygen atom to simulate the intermolecular contacts present in the crystal structure, the total charge being zero. The atomic coordinates were taken from the neutron structure, the water molecule was placed at the same position as the

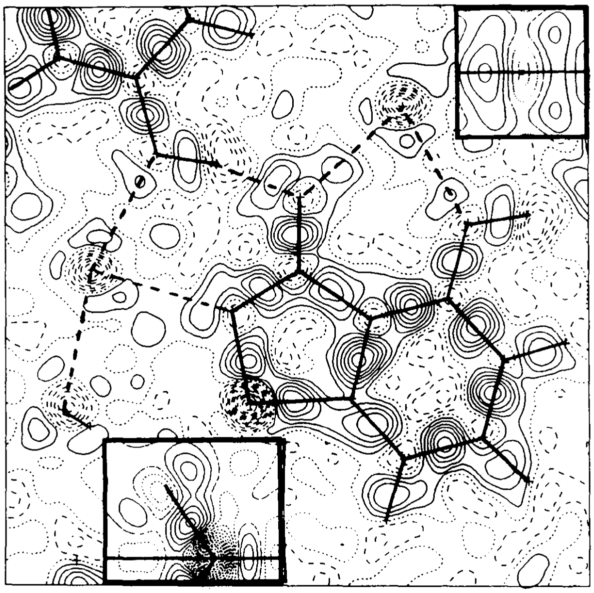

Fig. 2. X—X deformation density in the molecular plane and sections through O(3) perpendicular to the C(3)—O(3) bond (above right) and through O(1S), S(1) and O(1S′) (below left). The straight dashed lines mark the hydrogen bond O(5)—H(5)···O(3) and some Na$^+$ coordinations. Horizontal solid lines mark the projections of the molecular plane. Atomic parameters of non-H atoms are calculated from high-order X-ray data, those of H atoms from neutron measurement. $[(\sin\theta)/\lambda]_{\rm max}$ = 0·70 Å^{-1}. Contour lines are at 0·1 e Å^{-1} intervals with the zero and negative contours dashed.

hydroxyl group of the neighbouring anion in the experimental structure. As a reference additional calculations of the structure and charge distribution of four small molecules were carried out with different charges assumed at the carbonyl oxygen (Table 7).

The *ab initio* calculations were performed using the *GAUSSIAN*86 program (Frisch *et al.* 1984). The results are shown in Table 7 and Figs. 3 and 4. Obviously the deformation density of the complete molecule and the fragment are nearly identical (Figs. 3*a*,*b*). Therefore it seems justifiable to replace calculations of the complete molecule by those of the fragment.

Table 7. *Results of the ab-initio calculations*

Molecule, basis	Charge at O(3) (or equivalent)	C—O bond length (Å)
H_2CO, 6-31G*	−0·35	1·178
HCOO , 6-31G*	−0·64	1·227
HCONH , 6-31G*	−0·65	1·230
H_3CO , 6-31G*	−0·83	1·307
Fragment, 3-21G*	−0·69	
Fragment, 6-31G*	−0·69	
UH-AF 50, 3-21G*	−0·68	

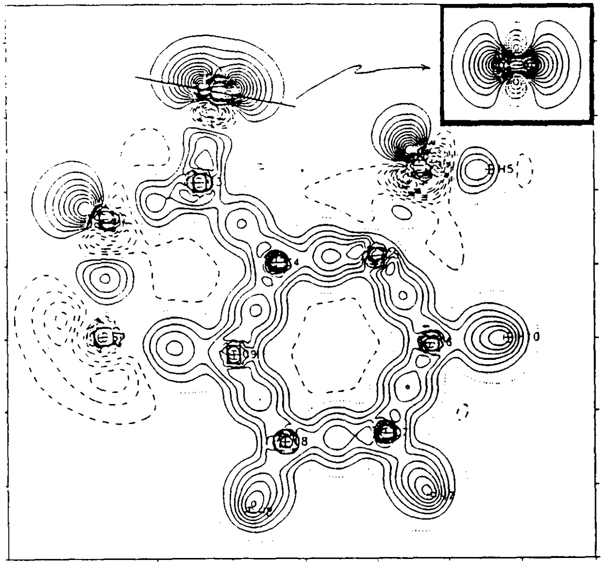

The calculated atomic charges at the carbonyl oxygen of both the molecule and the fragment are very similar to those of the acetic acid anion or the formamide anion. This corresponds with a good agreement of the theoretically calculated C—O bond of these anions with the experimental value 1·245 (1) Å for C(3)—O(3).

The atoms O(3), N(2) and O(1S) of the 'glucophore' region all take part in sodium coordination and/or hydrogen bonds. The influence of these bonds on the electron deformation density can be studied

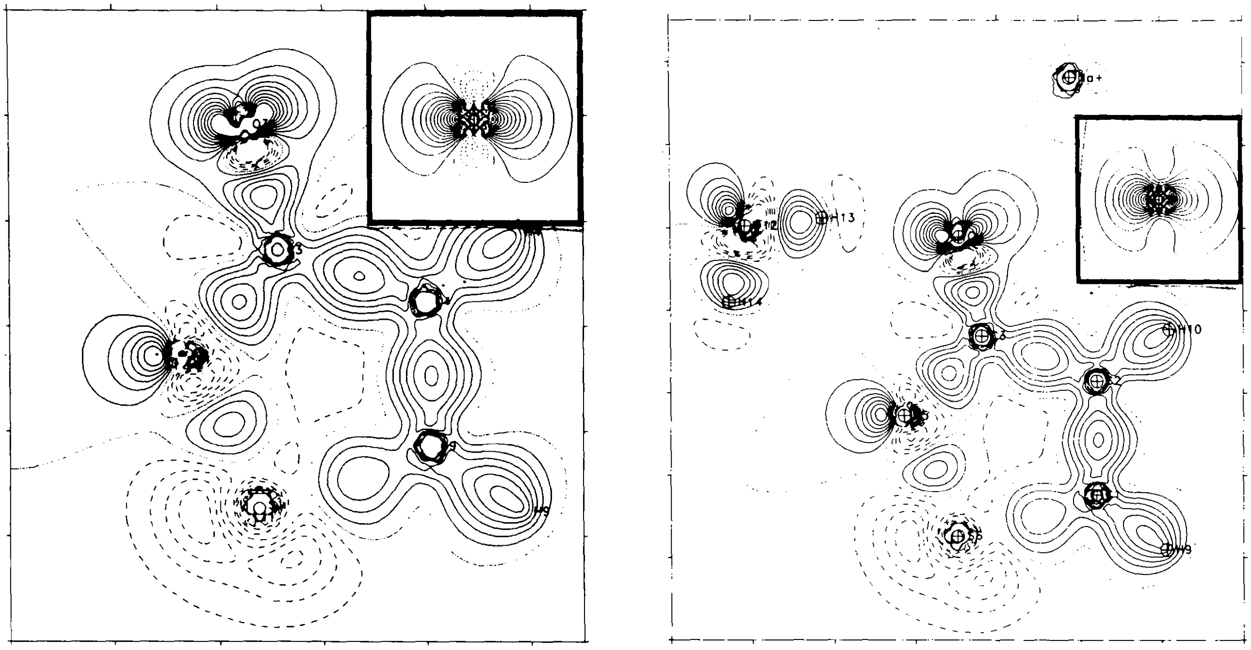

Fig. 3. EDD maps from the *ab initio* calculations of (*a*) UH-AF 50, basis 3-21G*, (*b*) the five-membered ring fragment anion of UH-AF 50, basis 6-31G*, (*c*) as in (*b*) plus one sodium cation and one water molecule. Contour lines as in Fig. 2. The molecular plane and sections through the oxygen atom perpendicular to the C—O bond are shown.

by comparison with the theoretical calculations. The lone-pair peaks of the theoretical maps within the molecular plane are more pronounced than those of the experimental electron deformation density. Figs. 3(*b*) and 3(*c*) show that the sodium coordination and the hydrogen bond induce a loss of symmetry at the lone pairs of O(3). The lone pair in the hydrogen-bond direction does not change visibly whereas the lone pair pointing towards the sodium cation becomes more diffuse and weaker. This is found more clearly in the sections along the hydrogen bond and along the sodium coordination (Fig. 4). In the experimental density map the sodium cations also seem to have a weakening influence on the lone pairs. This is found in one of the lone pairs of O(3) and in the lone pairs of O(5), N(2) and O(1*W*), but not in the lone pairs of O(1S) (Fig. 2).

In the O(5)—H(5)···O(3) hydrogen bond there is a charge deficiency between the hydrogen atom and the oxygen lone pair. The same is true for the theoretical map. This is consistent with an interaction for hydrogen bonding which is primarily electrostatic (Olovsson, 1982).

With a length of 1·245 (1) Å the bond C(3)—O(3) should have partial double-bond character. This is confirmed by the height of the bond peak compared to the single-bond C(5)—O(5) bond peak and by *ab initio* calculations for some small reference molecules (Table 7). The sodium cation is sixfold coordinated by O(3), O(5), N(2), O(1*W*), O(1S), and O(1S′) (Table 6). The first four atoms are situated in the molecular plane together with Na$^+$. Within the molecular plane Na$^+$ is surrounded by positive electron deformation density which is slightly above the noise level. O(1S) and O(1S′), which are above and below the molecular plane, have the shortest contacts to the Na$^+$ cation; nevertheless, no density maxima are observed outside of the plane (Fig. 4*b*).

Judged from the experimental deformation density the hydroxyl group O(5)—H(5) is positively charged.

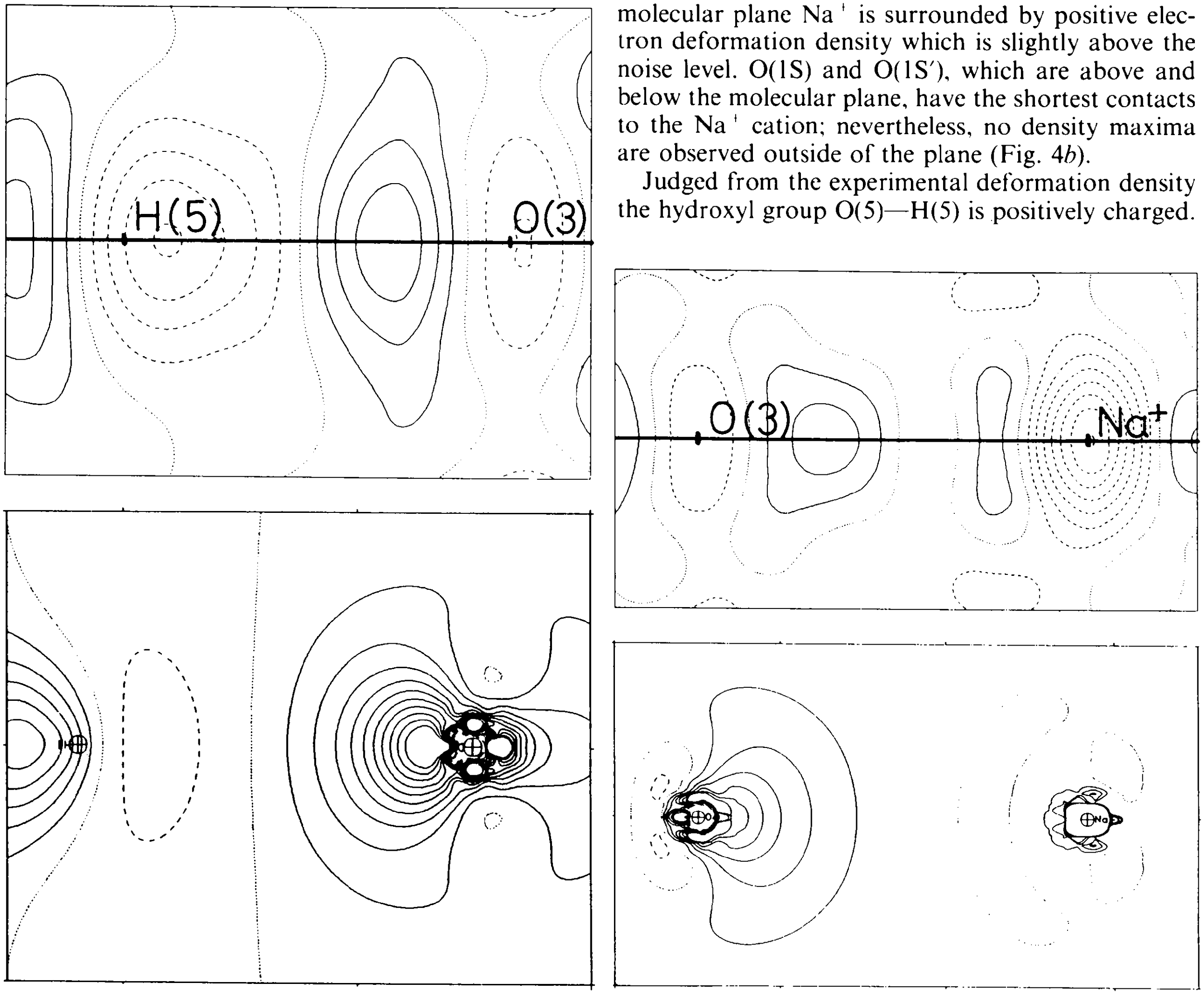

(*a*) (*b*)

Fig. 4. Sections of the experimental (above) and theoretical (below) deformation densities perpendicular to the molecular plane containing the atom O(3). The theoretical densities include Na$^+$ and water. The projection of the molecular plane is indicated by a horizontal line in the experimental maps. Fig. 1 shows the positions of these sections. Contours as in Fig. 2. (*a*) Hydrogen bond H(5)/H···O(3), (*b*) coordination O(3)···Na$^+$.

Some of the electron density may have been transferred to the Na^+ cation.

Concluding remarks

The influence of sodium cations on coordinated lone-pair deformation densities is too strong to be neglected. In the case of UH-AF 50 NA the sodium cation seems to weaken the densities of most of the lone pairs. The influence of hydrogen bonds may be much lower. Therefore it would be interesting to measure the deformation density of the ammonium or amine salts of the title compound.

This work has been funded by the German Federal Minister for Research and Technology (BMFT) under contract No. 03-LU1 FUB-0-F1-55 and by the Fonds der Chemischen Industrie. We thank Dr Hans-Ullrich Wagner, Institute of Organic Chemistry, University of Munich, for helpful advice.

References

Frisch, M. J., Binkley, J. S., Schlegel, H. B., Raghavachari, K., Melius, C. F., Martin, R. L., Stewart, J. J., Bobrowicz, F. W., Rohlfing, C. M., Kahn, L. R., Defrees, D. J., Seeger, R., Whiteside, R. A., Fox, D. J., Fluder, E. M. & Pople, J. A. (1984). *GAUSSIAN86*. Carnegie-Mellon Quantum Chemistry Publishing Unit, Pittsburgh, PA, USA.

Keller, E. (1988). *SCHAKAL88. A FORTRAN Program for the Graphic Representation of Molecular and Crystallographic Models*. Univ. of Freiburg, Germany.

Olovsson, I. (1982). *Croat. Chem. Acta*, **55**, 171–190.

Rudert, R., Buschmann, J., Luger, P., Gregson, D. & Trummlitz, G. (1988). *Acta Cryst.* C**44**, 1083–1086.

Rudert, R., Buschmann, J., Luger, P., Gregson, D. & Trummlitz, G. (1989). *Acta Cryst.* C**45**, 1013–1015.

Schomaker, V. & Trueblood, K. N. (1968). *Acta Cryst.* B**24**, 63–76.

Stewart, J. M. & Hall, S. R. (1986). Editors. *The XTAL System of Crystallographic Programs*. Tech. Rep. TR-1364.2. Computer Science Center, Univ. of Maryland, College Park, Maryland, USA.

Stewart, R. F., Davidson, E. R. & Simpson, W. T. (1965). *J. Chem. Phys.* **42**, 3175–3187.

Wang, Y. & Liao, J. H. (1988). *Acta Cryst.* B**45**, 65–69.

Zachariasen, W. H. (1967). *Acta Cryst.* **23**, 558–564.

Acta Cryst. (1991). B**47**, 910–917

Electron-Density Distribution in *lel*$_3$- and *ob*$_3$-Tris(*trans*-1,2-diaminocyclohexane)cobalt(III) Nitrate Trihydrate at 120 K

By Mitsuo Morooka, Shigeru Ohba* and Yoshihiko Saito

Department of Chemistry, Faculty of Science and Technology, Keio University, Hiyoshi 3-14-1, *Kohoku-ku, Yokohama* 223, *Japan*

and Hiroshi Miyamae

Department of Chemistry, Faculty of Science, Josai University, Keyakidai 1-1, *Sakado-shi, Saitama* 350-02, *Japan*

(*Received* 19 *February* 1991; *accepted* 11 *June* 1991)

Abstract

The electron-density distribution in two optically active Co^{III} complexes with *trans*-1,2-diaminocyclohexane (chxn) as a bidentate ligand have been investigated by the multipole-expansion method based on X-ray intensities collected at 120 K with Mo $K\alpha$ radiation (λ = 0·71073 Å). Crystals of the *lel*$_3$- and *ob*$_3$-conformers are isotypic and hexagonal $P6_3$, $Z = 2$, R = 0·038 and 0·033 for 3916 and 1831 reflections, respectively. $[\mathrm{Co}(R,R\text{-chxn})_3](\mathrm{NO}_3)_3.3\mathrm{H}_2\mathrm{O}$, M_r = 641·6, $F(000)$ = 684. (I): $\Delta(\lambda\lambda\lambda)$-complex (*lel*$_3$-isomer), a = 12·998 (3), c = 9·973 (3) Å, V = 1459·2 (8) Å^3, D_x = 1·46 Mg m^{-3}, μ = 0·653 mm^{-1}. (II): $\Lambda(\lambda\lambda\lambda)$-complex (*ob*$_3$-isomer), a = 13·192 (1), c = 9·787 (2) Å, V = 1475·0 (5) Å^3, D_x = 1·44 Mg m^{-3}, μ = 0·646 mm^{-1}. The aspherical 3*d*-electron distribution around the Co atom is essentially the same as that of the octahedral complex for both isomers and significant chirality was not observed. The necessity of phase improvement for the deformation density around the Co atom in the non-centrosymmetric structures depends on the symmetry of the multipole densities. The features of the multipole density, hexadecapole y_{40}, are not smeared by the use of the independent atom model (IAM) phase because the phase of the y_{40} contribution to the structure factor coincides with that of the cobalt monopole. On the other hand, the features of y_{43} are much affected by the phase error. Incompleteness of the Fourier series within the $(\sin\theta/\lambda)_{\max}$ in the

---

* To whom correspondence should be addressed.

0108-7681/91/060910-08$03.00 © 1991 International Union of Crystallography